

Experimental Indoor Validation of Weak Intensity Fluctuations over Free-Space Optical Communication Link

Dejan N. Milić¹, Daniela M. Milović¹, Jelena A. Anastasov¹

Abstract: In this paper, we present experimental results for characterizing turbulence phenomena in free-space optical (FSO) communication under laboratory controlled conditions. Collected data is used for statistical determination of the probability density function (PDF) of irradiance signal fluctuations. In literature, there are a number of empirical models for variety of turbulence regimes. Thus, obtained PDF is compared with selected models from the bibliography in order to describe properly statistical properties of real turbulent channel and help improving of FSO system performance calculation. In overall, analysis has shown that the results obtained under given constraints fit well with the exponentiated Weibull turbulence model.

Keywords: Free space optics, Probability Density Function (PDF), Scintillation, Turbulence.

1 Introduction

While increased requirements in the field of wireless communication exhaust the capabilities of the radio frequency spectrum, optical wireless communication (OWC) can offer access to a wealth of spectrum in the optical domain, thereby resolving problems with the radio spectrum crunch [1 – 2]. In addition, the OWC systems have been developed as a response to growing need for a high-speed wireless communications. Fixed optical atmospheric links are already a separate commercial segment in the local and metro networks. Further, a significant area that has been studied is the communication between the ground stations and space satellite [3]. Potentially, the free space optics (FSOs) technology can be used to bridge the last-mile problem, bring internet to rural areas, and interconnect mobile base stations. Global acceptance of laser based FSO communication is slow because of strong attenuation of signals due to bad weather and low visibility conditions [4]. Unfavorable atmospheric conditions can degrade the system performance significantly. An absorption and scattering of light in the fog,

¹University of Niš, Faculty of Electronic Engineering, Aleksandra Medvedeva 14, 18106 Niš, Serbia;
E-mails: dejan.milic@elfak.ni.ac.rs, daniela.milovic@elfak.ni.ac.rs, jelena.anastasov@elfak.ni.ac.rs.

clouds, dust, and smoke, significantly attenuate laser beams that propagate through the atmosphere, and limit the optical link performance and availability [1, 2, 4, 5]. Large variations of attenuation can incapacitate the links and cause relatively long outage periods.

The performance of an optical system operating over turbulence conditions can be deduced from an adequate mathematical model for the probability density function (PDF) of the irradiance signal (scintillation) [2, 5]. According to this, the main goal on the study of optical wave propagation through free-space was the identification of a tractable PDF for the irradiance under all intensity fluctuation regimes. Over the years, various theoretical models have been proposed [4, 6–12], but still there is no unique distribution capable to describe all turbulence strengths under all aperture averaging conditions. Among them, there are lognormal (LN) [4], inverse Gaussian model as a less complex alternative to LN [6], so-called Beckmann model [7], the Gamma-Gamma (G-G) [8], exponentiated Weibull (EW) [9–10] and Malaga (M) model [11–12]. The LN model have shown a good fit for weak irradiation fluctuations while G-G was introduced as an excellent model for medium to high irradiance regimes and also a good approximate alternative for weak turbulence conditions. Regardless to the fact that the Beckmann distribution showed a good fit to experiments, its inconvenient mathematical form made it unfavorable for wider utilization. More recently, as an alternative to LN and G-G distributions, EW and M models were proposed. The EW distribution offered favorable properties for describing FSO links under weak and moderate turbulence under all aperture averaging conditions. The M model was proposed as unifying statistical model effective for both plane and spherical waveform propagation under all irradiance fluctuations.

Some of the strategies that can be used to overcome scintillation effects include increase of transmitted optical power, use of different wavelengths, multiple beams and/or multiple receivers. In any case, it is very important to accurately describe and model the turbulent channel, including its statistical properties, in order to suppress its negative effects and improve the performance of treated optical system. According to this, EW has been proposed as fitable PDF for describing realistic turbulence channel between the rooftops of two buildings along a medium density residential terrain in Barcelona [9–10]. Experimental analysis along with simulation results and comparison with other turbulence models has been reported. Further on above topic, the experimental validation of FSO channel in a coastal environment by modeling the channel attenuation coefficient depending on the air temperature, relative humidity and dew point have been reported [13]. Determination of rain attenuation parameters for FSO link in tropical rain [14], and experimental verification of fog models in turbulent channel under laboratory conditions have also been presented in literature [15].

Unlike [9–10], we perform experimental analysis of atmospheric scintillation caused by turbulence in indoor scenario, under laboratory controlled conditions. Namely, we have used the short turbulence chamber created by PVC pipes, 3 m in total, for experimental purposes. Our original results confirm that EW distribution fits well for describing weak turbulence conditions either in indoor or in outdoor environment. In general case, information is transmitted by modulating the laser beam. During propagation, the beam is disturbed by further undesired modulation of the random fluctuations of atmospheric properties. In order to correctly receive the information, the received signal is demodulated i.e. the useful information-bearing modulated signal is separated from the random modulated signal caused by atmospheric scintillations. Obtained results are processed and final experimental data is compared with the matching results already proposed in literature. Detailed discussion and concluding remarks are given in final section.

2 Laboratory Setup

Experimental setup suitable for the purpose of verifying theoretical distributions has been assembled in the Laboratory for telecommunication systems at University of Niš, Faculty of Electronic Engineering. The setup consists of three main parts:

- light source;
- turbulence chamber;
- photodetector with acquisition system.

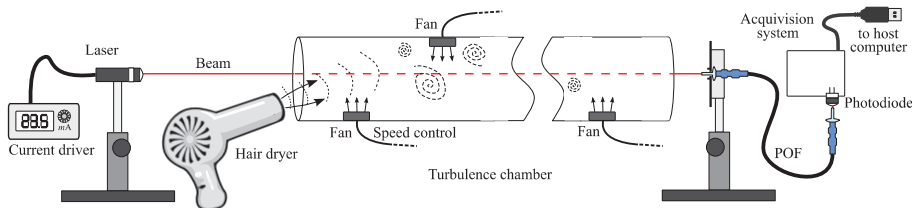


Fig. 1 – Schematic representation of experimental setup.

We have used a semiconductor laser as a light source. Wavelength of the emitted light is 650 nm, which is in the red part of the visible spectrum, so the beam is visible and therefore its position can be easily adjusted. A custom driver has been designed and realized for the purpose of driving the laser with constant current that can be adjusted according to our needs. Injection current can be adjusted from zero to 50 mA, which corresponds to emitted optical power between zero and 10 mW. Lasing threshold has been observed at 10.5 mA at room temperature. Optical power has been measured using thermopile detector

available at the laboratory, and measurements confirmed good stability of emitted power after allowing enough time for the temperature to stabilize. Stability has further been tested using PIN photodiode detector as a part of initial testing of acquisition system, which will be discussed later.

We have built the turbulence chamber using multiple PVC pipes connected to each other, totaling 3 m in length. Inner diameter of the chamber is 20 cm. Along the chamber, a set of four fans is distributed, each fan being directed perpendicularly to chamber axis, i.e. to beam propagation direction. The fans are controlled individually in terms of the voltage supplied, resulting in the control of speed at which they are turning, and in turn, the air flow speed they produce. Additionally, temperature gradient is added using a simple hair dryer fan blowing hot air at one end of the turbulence chamber. Besides the thermal gradient, hair dryer adds the turbulence strength by its additional air flow. By changing the angle at which the hair dryer fan is directed in relation to laser beam propagation path, different turbulence conditions can be achieved, owing it to different temperature gradients and air flow conditions.

Laser beam is incident on a connector face of a multi-mode plastic optical fiber (POF), and then guided to a PIN photodiode receiver via a short length of the fiber. Optical receiver is designed and built in the laboratory, and connected to an acquisition system. The acquisition system is based on an Arduino platform, and it uses its internal ADC (analogue-to-digital converter) in order to sample the analogue signal from the receiver. Also, after each conversion, the micro-controller transfers the data via USB connection to a host computer where it is stored for later processing.

3 Interpretation of Experimental Data

At first, we tested the transmitter/receiver combination without any turbulence in order to establish the baseline levels. Our receiver is of high-impedance type, although we have decided not to use very high resistance load, in order to obtain wider input bandwidth. The ADC resolution is 4.9 mV, which is translated into input-referred current resolution of 40 nA, with receiver gain of 120, and the load resistor of 1 kΩ. The receiver is limited by the noise level of pre-amplifier, which is specified at $40 \text{ nV}/\sqrt{\text{Hz}}$, and for the bandwidth under consideration it is translated into input-referred noise current of 16 nA. Therefore, the receiver noise level is bellow ADC resolution limit, and the receiver is able to precisely detect constant optical power.

The turbulence is often characterized by its normalized variance of irradiance fluctuations [5], or scintillation index, which is defined as

$$\sigma_I^2 = \frac{\text{E}[I^2]}{\left(\text{E}[I]\right)^2} - 1, \quad (1)$$

where I is irradiance at the receiving aperture, and $E[\cdot]$ denotes mathematical expectation operator [16]. Irradiance is directly proportional to measured photo current, and therefore proportional to the acquisition system output X . Moments of the stochastic process X are estimated from its time series $\{x_i, 1 \leq i \leq N\}$ as averages

$$E[X^k] = \frac{1}{N} \sum_{i=1}^N x_i^k, \quad (2)$$

and consequently scintillation index is simply $\sigma_I^2 = E[X^2]/(E[X])^2 - 1$, as long as the process is ergodic.

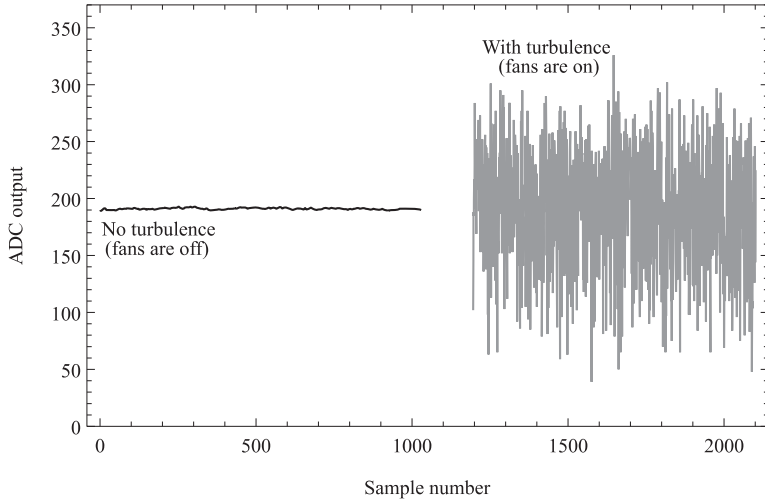


Fig. 2 – Partial data captured while fans were turned off and on. Scintillation index when the fans are turned on is $\sigma_I^2 = 0.0749$, based on a full data set.

Fig. 2 shows two series of ADC output samples for the case without turbulence, i.e. all fans turned off, versus the case of fans turned on. Even when the fans are off, there are slight variations of the received optical power. We attribute those to combined influence of relative intensity noise and the free floating particles of dust interfering with the beam, as the experiment is not conducted in controlled atmosphere.

Total variance of signal $\sigma_0 = (1/N \sum_{i=1}^N (x_i - E[X])^2)^{1/2}$, in this particular case is determined to be only 1.3 ADC quants and the corresponding scintillation index is $\sigma_I^2 = (\sigma_0 / E[X])^2 = 0.000047$. Therefore, the setup is suitable for experimental analysis when scintillation index is above this value. On the other hand, this value is very small and the turbulence conditions that are of interest

exceed many times (or even many orders of magnitude), this low limit of measurable scintillation index.

As the fans are turned on in various combinations, different turbulence conditions are established, and the received signal levels show more or less variation. After collecting a large number of samples, the data is processed in order to obtain the signal statistical parameters. We are interested in probability distribution of the signal levels, and more specifically in the probability density function (PDF). In order to estimate the PDF, we construct a histogram from each series of samples, and then normalize the scale so the probability normalization condition can be met (Fig. 3). The PDF obtained in this way is further compared to theoretical models.

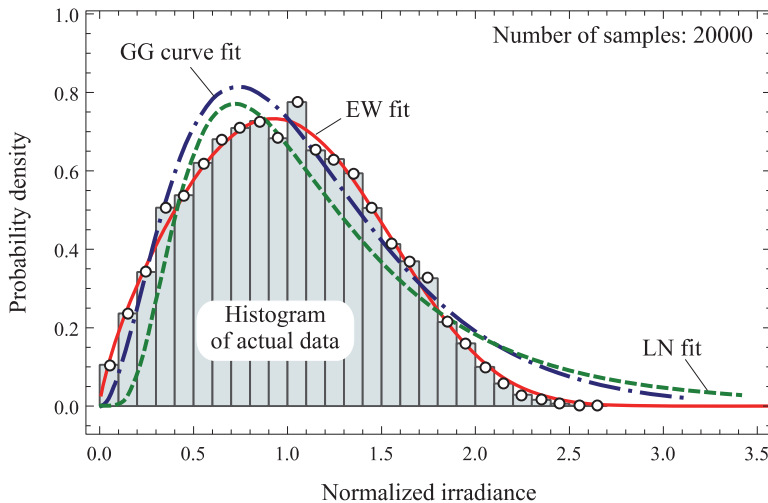


Fig. 3 – Histogram of collected data, normalized for estimating the PDF. Fitted curves corresponding to LN, G-G using Rytov theory, and EW models are also shown. Scintillation index from the data series is $\sigma_i^2 = 0.2375$.

3 Theoretical Models

The ideal theoretical model of irradiance would be valid in all regimes of turbulence, for any receiving aperture size. It would have a closed mathematical form, and its parameters would be directly related to physical atmospheric quantities. Unfortunately, such a perfect model is not yet known, if it exists. Some of the most widely used models are described in this section, and compared to our experimental data.

The LN model [1, 4] is the most used model under weak irradiance fluctuations. It is obtained as a first-order Rytov approximation, and the PDF for its intensity fluctuations is

$$p_I(x) = \frac{1}{x\sigma_i\sqrt{2\pi}} \exp\left[-\frac{(\log x + \sigma_i^2/2)^2}{2\sigma_i^2}\right], \quad x > 0, \quad (3)$$

where σ_i^2 is the variance of the normalized log-irradiance.

Moreover, $E[\log I] = -\sigma_i^2/2$. Scintillation index corresponding to LN model is $\sigma_{I_{LN}}^2 = -1 + \exp(\sigma_i^2)$.

Nakagami- m model for radio propagation and its extension by Rice have been applied in description of optical wave propagation [7] as Backmann/modified Rician-MR turbulence model. Normalized intensity I is expected to have the following PDF

$$p_I(x) = \frac{1}{b} \exp\left(-\frac{1+x}{b}\right) I_0\left(2\frac{\sqrt{x}}{b}\right), \quad b, x > 0, \quad (4)$$

with $I_0(\cdot)$ being the modified Bessel function of the first kind. The model is valid for scintillation indices below 2.

Theoretical scintillation index is: $\sigma_{I_{MR}}^2 = -1 + (2/(1+1/b)^2)L_2(-1/b)$, where $L_2(x)$ is the second order Laguerre polynomial $L_2(x) = x^2/2 - 2x + 1$.

The G-G turbulence model [2, 8] represents a double stochastic model based on a scintillation theory. It considers irradiance fluctuation as a modulation process resulting from the small-scale and large-scale turbulent eddies. Each effect is modelled by gamma distribution, and thus the name. Resulting PDF of the normalized intensity I is

$$p_I(x) = \frac{2(\alpha\beta)^{(\alpha+\beta)/2}}{\Gamma(\alpha)\Gamma(\beta)} x^{(\alpha+\beta)/2-1} K_{\alpha-\beta}(2\sqrt{\alpha\beta x}), \quad \alpha, \beta, x > 0, \quad (5)$$

where $\Gamma(\cdot)$ is Gamma function and $K_v(\cdot)$ is the second order Bessel function [16]. Parameters α and β are effective numbers of large-scale and small-scale scatterers, respectively, directly related to atmospheric parameters C_n^2 and l_0 . It can be shown that scintillation index value can be evaluated as $\sigma_{I_{GG}}^2 = (1+1/\alpha)(1+1/\beta) - 1$.

The M-distribution model [11–12] is proposed as a more general model that includes, as special cases, almost all valid models and theories that have been previously proposed in the bibliography. We choose a general formulation of the

model, which is expressed in the form of an infinite series, but imposes no restriction on the parameter values

$$p_I(x) = A^{(G)} \sum_{k=1}^{\infty} a_k^{(G)} x^{\frac{\alpha+k-1}{2}} K_{\alpha-k} \left(2 \sqrt{\frac{\alpha x}{\gamma}} \right), \quad \alpha, \theta, \gamma, x > 0, \quad (6)$$

where

$$A^{(G)} = \frac{2}{\gamma \Gamma(\alpha)} \left(\frac{\alpha}{\gamma} \right)^{\frac{\alpha}{2}} \left(\frac{\gamma \theta}{\gamma \beta + 1} \right)^{\theta}, \quad a_k^{(G)} = \frac{(\theta)_{k-1} (\alpha \gamma)^{\frac{k}{2}}}{[(k-1)!]^2 \gamma^{k-1} (\gamma \theta + 1)^{k-1}}, \quad (7)$$

with $(t)_i$ being the Pochhammer symbol and θ being the shape parameter of Nakagami- m distribution.

Furthermore, the EW model [9–10] is shown to offer an excellent fit to simulation and experimental data under all aperture averaging conditions, under weak and moderate turbulence conditions, as well as for point-like apertures. Another very attractive property of the distribution is the simple closed form expression of its respective PDF [9]

$$p_I(x) = \alpha \beta x^{\beta-1} \exp(-x^\beta) [1 - \exp(-x^\beta)]^{\alpha-1}, \quad \alpha, \beta, x > 0. \quad (8)$$

On the other hand, the analytical derivation of the distribution parameters is rather a complex task; hence, a heuristic approach is used to obtain approximation to the EW parameters from atmospheric data. The scintillation index is

$$\sigma_{I_{EW}}^2 = \frac{\Gamma(1+2/\beta) g_2(\alpha, \beta)}{\alpha (\Gamma(1+1/\beta) g_1(\alpha, \beta))^2} - 1, \quad (9)$$

$$g_n(\alpha, \beta) = \Gamma(\alpha) \sum_{j=0}^{\infty} \frac{(-1)^j}{j! (j+1)^{1+n/\beta} \Gamma(\alpha-j)}. \quad (10)$$

5 Experimental Results and Discussion

By adjusting angles and speeds of the fans we have been able to obtain conditions that result in scintillation index values ranging from 0.0053 to 0.3614, and therefore classified as weak turbulence scintillation indices. Strong turbulence conditions require longer paths and/or stronger fans. Using the collected data, we have made numerical fits to the theoretical models listed in the previous section. Fitting is done with the least mean-square criteria using Levenberg-Marquardt algorithm [17].

The concluding remarks from Figs. 4 and 5 are listed below.

Contrary to expectations, the LN model demonstrated less than perfect fits in all but the weakest turbulence cases. This is especially important when the PDF tails are considered, as the tail probability bears high significance during

telecommunication systems' performance evaluation. In fact, among all of the models considered, LN model has performed as poorest when used to estimate the tail probabilities. It underestimates lower probability tail, overestimates the upper tail, and therefore is expected to give optimistic results for system performance, even under weak turbulence conditions.

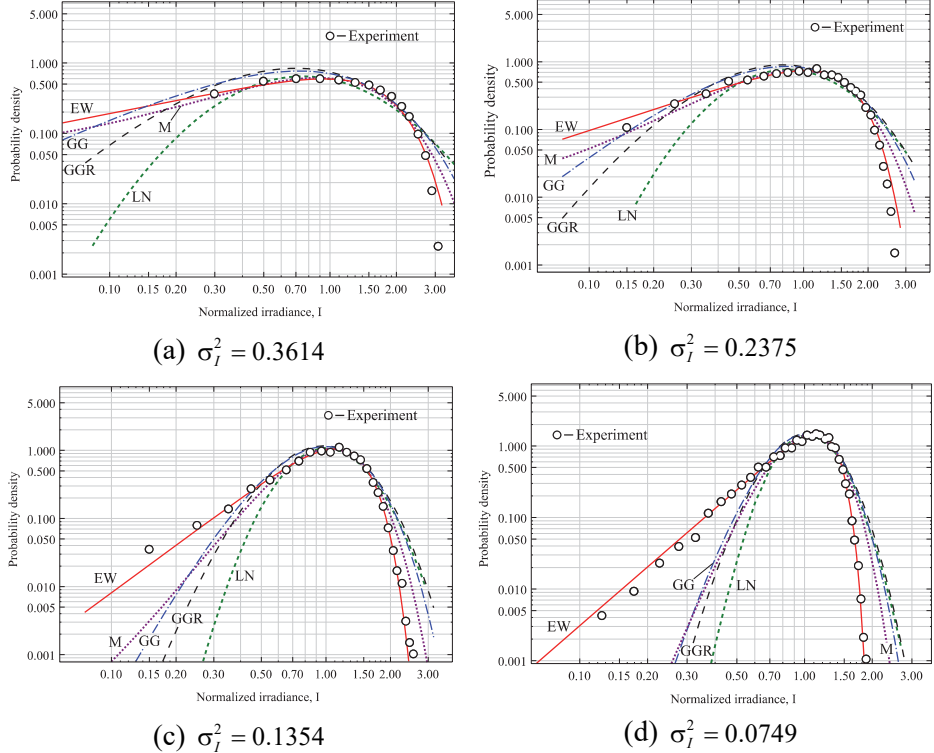


Fig. 4 – Experimental results for a range of weak turbulence conditions, compared to numerical fits using different theoretical models:
LN, GG, GGR: G-G using plain wave Rytov theory, M, EW.

Somewhat better results are obtained with G-G model. We have considered two cases: one corresponding to parameters according to Rytov theory for plane waves (GGR), and the other based on free choice of parameter values, designated (G-G). We have noticed that in the weakest turbulence conditions there is little difference between the two cases. As the scintillation index becomes larger, the G-G model shows better results, and the tail probabilities are better approximated when compared to the LN model. Free choice of the parameters gives better results, and our conclusion is that the plain wave Rytov approximation is not entirely valid for the conditions under testing. When the parameters in G-G model are taken into account independently, our results indicate that fitting values of

parameter α , corresponding to effective number of large-scale turbulent cells are much higher than the values for β , which corresponds to small-scale eddies. This is an indication that the beam can be considered partially coherent, and that the coherence length is relatively small, as indicated in [18].

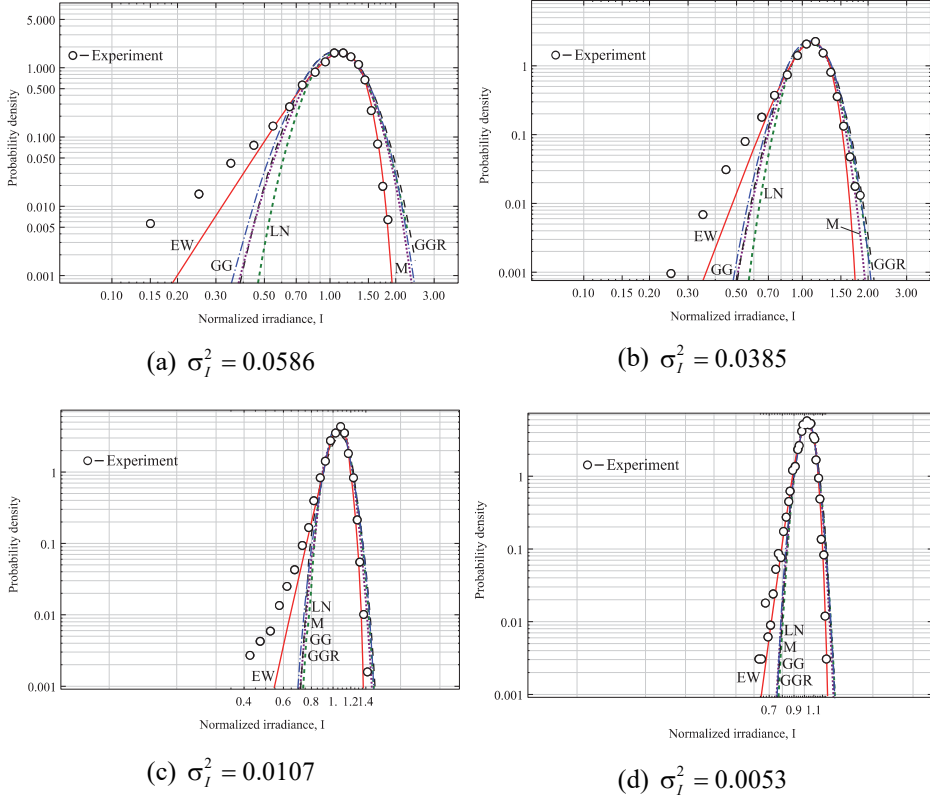


Fig. 5 – Experimental results for a range of weak turbulence conditions, compared to the numerical fits using different theoretical models: LN, GG, GGR, M, EW.

The M-distribution fitting results support this conclusion, with parameter α being very high, and the results obtained are very close to the MR model. However, added complexity of general M-model does not lead to significantly better fits, and the results are comparable to G-G model. On the other hand, there are significant numerical difficulties when trying to fit the weak turbulence data to this general model, as the required values for α and β parameters are very high. Similar problems have also been observed for general G-G model under weak turbulence conditions.

M-distribution model enables characterization of a number of different propagation conditions including line-of-sight (LOS) components, components

coupled to LOS, and independent components. In our particular case, according to the derivation details [11] we deduce that there is a low correlation between LOS components and coupled LOS components, and also low scintillations of direct LOS components. In overall, M model was not suitable for the particular conditions in the experiment.

The EW distribution, on the other hand, has demonstrated much better fits to our experimental results. We have used independent choice for the distribution parameters, as there is limited theoretical background available for parameter derivations under different atmospheric conditions. Upper tail probabilities approximate collected data very well, while the lower tail approximation is generally good, but with some subtle variations. As for the main probability mass, the level of agreement between the fitted EW curves and experimental data is very good, which is demonstrated by the results shown in Fig. 3.

Again, the results presented in Table 1 show the largest deviation between the LN model and the results we obtained through the experiment. Namely, the Table shows scintillation index comparison between the existing theoretical results and experimental data. The smallest deviation expressed in percentages can be noticed in comparison with EW turbulence scintillation index.

Table 1

Scintillation index σ_I^2 from experimental data versus the scintillation indices from the best fits using different theoretical models. The relative differences to the experimental results are also shown in percentage.

σ_I^2	LN	[%]	GGR	[%]	GG	[%]	M	[%]	EW	[%]
0.3614	1.099	+204.1	0.6651	+84.0	0.542	+50.0	0.5010	+38.6	0.3754	+3.9
0.2375	0.4316	+81.7	0.3845	+61.9	0.3300	+38.9	0.3108	+30.9	0.2462	+3.7
0.1354	0.1589	+17.4	0.1619	+19.6	0.1508	+11.4	0.1411	+4.2	0.1296	-4.3
0.0749	0.0762	+1.7	0.0823	+9.9	0.0795	+6.1	0.0805	+7.5	0.0780	+4.1
0.0586	0.0558	-4.8	0.0583	-0.5	0.0569	-2.9	0.0530	-9.6	0.0546	-6.8
0.0385	0.0315	-18.2	0.0324	-15.9	0.0329	-14.5	0.0307	-20.3	0.0316	-17.9
0.0107	0.0086	-19.6	0.0088	-17.8	-	-	-	-	0.0094	-12.1
0.0053	0.0049	-7.5	0.0050	-5.7	-	-	-	-	0.0052	-1.9

The established theoretical models do not cover fully the range of conditions realized in our experiment, somewhat in contrast with level of agreement reported by other authors for their simulation data. There are multiple reasons for this disagreement, some of the most important being:

- we don't provide the uniform turbulence conditions over the whole beam propagation path;

- the turbulence chamber has walls that impose boundary conditions not present in the open atmosphere;
- the size of large turbulent eddies is limited by the chamber geometry;
- the coherence length is relatively short, and the beam is partially coherent;
- the beam quality is not very high and the profile differs from ideal Gaussian shape.

6 Conclusion

Our experimental setup has demonstrated ability to properly characterize the propagation effects under laboratory environmental conditions. The analysis showed that collected data supports EW distribution as an adequate mathematical model for the measured results under given constraints. On the other hand, the distribution parameters that provide good fits are determined purely from mathematical manipulations and it is not clear whether a direct relation could be made to the propagation medium parameters. Therefore, more work should be directed towards establishing clear theoretical background for using the EW distribution. Primarily, the distribution parameters should be put into perspective with physical properties of the propagation medium. Moreover, the turbulence conditions in the described laboratory environment are only roughly representative of atmospheric conditions encountered in typical free-space optical communication systems.

7 Acknowledgment

This work has been supported by the Ministry of Education, Science and Technological Development of the Republic of Serbia.

7 References

- [1] V. I. Tatarskiy: Wave Propagation in Turbulent Atmosphere, Nauka, Moscow, 1967. (in Russian)
- [2] L. C. Andrews, R. L. Philips: Laser Beam Propagation through Random Media, 2nd Edition, Spie Press, Bellingham, WA, 2005.
- [3] M. Toyoshima, H. Takenaka, Y. Takayama: Atmospheric Turbulence-Induced Fading Channel Model for Space-to-Ground Laser Communications Links, Optics Express, Vol. 19, No. 17, August 2011, pp. 15965 – 15975.
- [4] X. Zhu, J. M. Kahn: Free-Space Optical Communication through Atmospheric Turbulence Channels, IEEE Transactions on Communications, Vol. 50, No. 8, August 2002, pp. 1293 – 1300.
- [5] L. C. Andrews, R. L. Philips, C. Y. Young: Laser Beam Scintillation with Applications, Spie Press, Bellingham, WA, 2001.
- [6] N. D. Chatzidiamantis, H. G. Sandalidis, G. K. Karagiannidis, M. Matthaiou: Inverse Gaussian Modeling of Turbulence-Induced Fading in Free-Space Optical Systems, Journal of Lightwave Technology, Vol. 29, No. 10, May 2011, pp. 1590 – 1596.

- [7] J. H. Churnside, S. F. Clifford: Log-Normal Rician Probability-Density Function of Optical Scintillations in the Turbulent Atmosphere, *Journal of the Optical Society of America A*, Vol. 4, No. 10, October 1987, pp. 1923 – 1930.
- [8] M. A. Al-Habash, L. C. Andrews, R. L. Phillips: Mathematical Model for the Irradiance Probability Density Function of a Laser Beam Propagating through Turbulent Media, *Optical Engineering*, Vol. 40, No. 8, August 2001, pp. 1554-1562.
- [9] R. Barrios, F. Dios: Exponentiated Weibull Distribution Family under Aperture Averaging for Gaussian Beam Waves, *Optics Express*, Vol. 20, No. 12, May 2012, pp. 13055 – 13064.
- [10] R. Barrios, F. Dios: Exponentiated Weibull Model for the Irradiance Probability Density Function of a Laser Beam Propagating through Atmospheric Turbulence, *Optics & Laser Technology*, Vol. 45, February 2013, pp. 13 – 20.
- [11] A. Jurado-Navas, J. M. Garrido-Balsells, J. F. Paris, A. Puerta-Notario: A Unifying Statistical Model for Atmospheric Optical Scintillation, *Numerical Simulations of Physical and Engineering Processes*, Edited by J. Awrejcewicz, IntechOpen, 2011.
- [12] J. M. Garrido-Balsells, A. Jurado-Navas, J. F. Paris, M. Castillo-Vazquez, A. Puerta-Notario: Novel Formulation of the M Model through the Generalized-K Distribution for Atmospheric Optical Channels, *Optics Express*, Vol. 23, No. 5, March 2015, pp. 6345 – 6358.
- [13] W. G. Alheadary, K.- H. Park, N. Alfaraj, Y. Guo, E. Stegenburgs, T. K. Ng, B. S. Ooi, M.- S. Alouini: Free-Space Optical Channel Characterization and Experimental Validation in a Coastal Environment, *Optics Express*, Vol. 26, No. 6, March 2018, pp. 6614 – 6628.
- [14] S. A. Al-Gailani, A. B. Mohammad, U. U. Sheikh, R. Q. Shaddad: Determination of Rain Attenuation Parameters for Free Space Optical Link in Tropical Rain, *Optik*, Vol. 125, No. 4, February 2014, pp. 1575 – 1578.
- [15] M. Ijaz, Z. Ghassemlooy, H. Le-minh, S. Zvanovec, J. Perez, J. Pesek, O. Fiser: Experimental Validation of Fog Models for FSO under Laboratory Controlled Conditions, *Proceedings of the IEEE 24th Annual International Symposium on Personal, Indoor, and Mobile Radio Communications (PIMRC)*, London, UK, September 2013, pp. 19 – 23.
- [16] I. S. Gradshteyn, I. M. Ryzhik, A. Jeffrey, D. Zwillinger: *Table of Integrals, Series, and Products*, 6th Edition, Academic Press, New York, 2000.
- [17] J. J. Moré: The Levenberg-Marquardt Algorithm: Implementation and Theory, *Proceedings of the Biennial Conference on Numerical Analysis*, Dundee, UK, June 1977, pp. 105 – 116.
- [18] O. Korotkova, L. C. Andrews, R. L. Phillips: Model for a Partially Coherent Gaussian Beam in Atmospheric Turbulence with Application in Lasercom, *Optical Engineering*, Vol. 43, No. 2, February 2004, pp. 330 – 341.